

# Specimen-specific tibial kinematics model for in vitro gait simulations

Tassos Natsakis<sup>1</sup>, Koen Peeters<sup>1</sup>, Fien Burg<sup>1,2</sup>, Greta Dereymaeker<sup>1</sup>,  
Jos Vander Sloten<sup>1</sup> and Ilse Jonkers<sup>2</sup>

## Abstract

Until now, the methods used to set up in vitro gait simulations were not specimen specific, inflicting several problems when dealing with specimens of considerably different dimensions and requiring arbitrary parameter tuning of the control variables. We constructed a model that accounts for the geometric dimensions of the specimen and is able to predict the tibial kinematics during the stance phase. The model predicts tibial kinematics of in vivo subjects with very good accuracy. Furthermore, if used in in vitro gait simulation studies, it is able to recreate physiological vertical ground reaction forces. By using this methodology, in vitro studies can be performed by taking the specimen variability into account, avoiding pitfalls with specimens of different dimensions.

## Keywords

In vitro gait simulations, gait analysis, tibial kinematics, specimen specificity

Date received: 20 February 2012; accepted: 13 September 2012

## Introduction

To systematically investigate the biomechanics of the musculoskeletal system, in particular, the foot, in vitro gait simulations demonstrate several advantages over in vivo experimentation and numerical model analysis: Numerical models are usually lacking experimental validation, whereas in vivo experiments are per definition limited to non-invasive interventions. The possibility to design studies that are highly invasive and repeatable is a major advantage of the in vitro simulations: During subsequent dissections, the effect of individual structures on foot function can be quantified as bone kinematics,<sup>1,2</sup> and joint contact area<sup>3</sup> or even intra-articular pressure distribution<sup>4,5</sup> can be measured. Furthermore, since the test condition is highly controllable, the effect of specific control parameters can be studied in isolation: Most often, the forces applied to the individual muscle tendons and loading conditions imposed to the foot are altered.

Our group developed an in vitro gait simulator,<sup>6</sup> which was comparable to previously published set-ups<sup>1,7–11</sup> and able to simulate stance phase at a physiologic speed (0.8 s; Figure 1). The gait simulator consists of a metallic frame, bearing a carriage with a set of six pneumatic actuators that can apply forces to the dissected muscle tendons. A force platform represents the ground and supports the specimen. The cadaveric

specimen is attached to the carriage and is supported by a platform. A servo-electric motor controls the carriage's horizontal progression. An actuator beyond the platform controls the vertical position of the platform and simulates the vertical distance of the knee to the ground. According to the imposed forces, the specimen then translates horizontally and rotates around a hinge joint, representing the knee. The combined action of the horizontal translation of the specimen and vertical translation of the platform allows simulating sagittal plane knee motion, further referred to as tibial kinematics.

A major challenge during in vitro gait simulation with this set-up is to determine the control input values for the tibial kinematics, especially with varying segment dimensions in different specimens. Other research groups already mentioned significant differences in kinematics in specimens of different dimensions, even if

<sup>1</sup>Department of Mechanical Engineering, Faculty of Engineering KU Leuven, Belgium

<sup>2</sup>Department of Kinesiology, Faculty of movement and rehabilitation sciences, KU Leuven, Belgium

### Corresponding author:

Tassos Natsakis, Department of Mechanical Engineering, Faculty of Engineering KU Leuven, Celestijnenlaan 300C, 3001 Heverlee, Belgium.  
Email: tassos.natsakis@mech.kuleuven.be

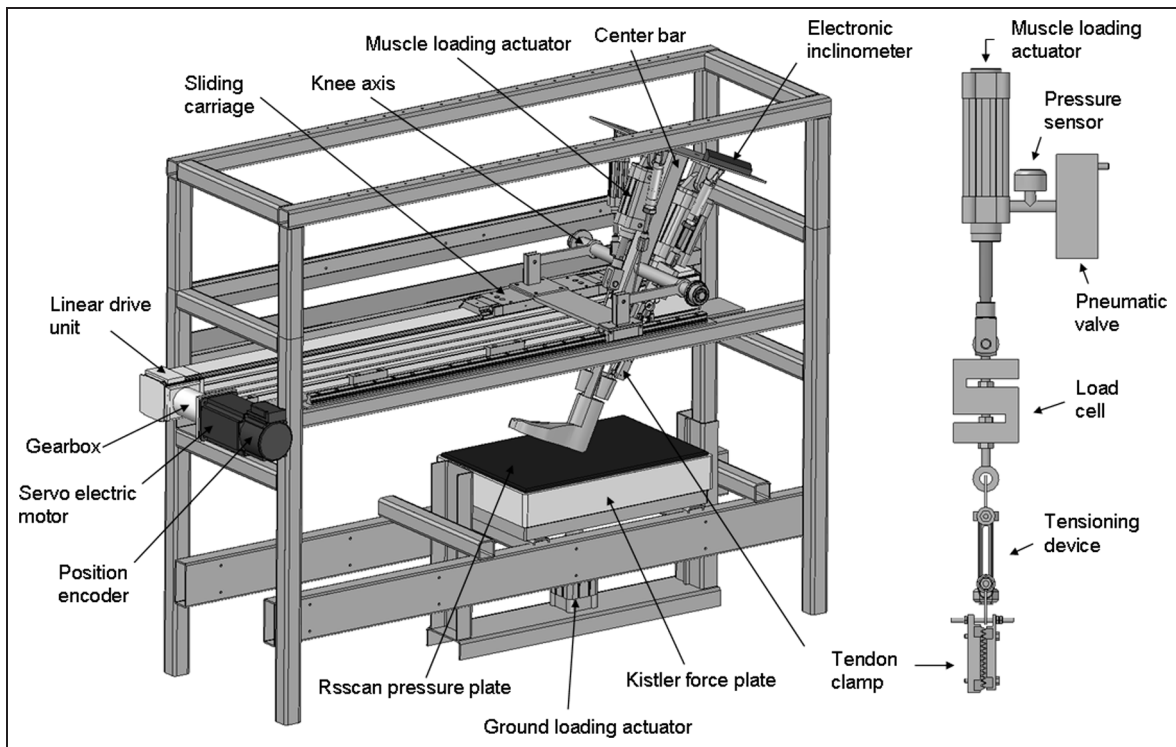


**Figure 1.** Diagram of the gait simulator. The key elements of the operation of the simulator are visible.

similar forces are applied to the tendons.<sup>7,11</sup> This is a result of applying prescribed tibial kinematics that does not reflect specimen morphology. To overcome this pitfall, arbitrary tuning of the tibial kinematics often precedes actual data collection. This inherently reduces the reproducibility of gait kinematics and kinetics over different specimens, thereby alleviating one of the major advantages of in vitro research. Intelligent selection of these control inputs is therefore crucial to achieve adequate reconstruction of in vivo foot–ankle kinematics in specimens with different geometric dimensions.

In this study, a geometric model for the calculation of control input of tibial kinematics is described, accounting for both tibial and foot geometry. This model is based on in vivo gait data and is implemented in the existing in vitro simulation set-up. The model performance is evaluated for in vivo as well as for in vitro conditions.

## Methods

### Model description

The goal of the geometric model is to calculate tibial kinematics based on geometric measures of the foot and tibia. The geometric model itself represents the tibia and foot by two rigid segments: The tibia is modelled as a rigid beam, whereas the foot is represented by a triangle. The two segments are linked at the ankle, which is modelled as a hinge joint. The geometric dimensions accounted for are the tibia length

( $l$ ), the foot length from heel to metatarsal head 1 ( $c$ ), the ankle height with respect to the ground ( $a$ ), the ankle distance from the heel ( $q$ ), the ankle distance from the metatarsal head 1 ( $m$ ), the dorsiflexion angle ( $\theta_i$ ) and the angle of the tibia with the vertical direction ( $\varphi_i$ ). The angle  $\omega_i$  is not a model input parameter but is used for simplifying the equations. It is calculated based on the other input parameters. The point ( $p$ ) is the most proximal end of the tibial segment and is further referred to as the knee (Figure 2).

Six temporal events during stance phase are defined (Figure 3): (1) heel-strike – foot positioned in plantar flexion relative to the tibia ( $\theta_1 = 97^\circ$ ) and the tibia positioned in a strike angle of  $\varphi_1 = 14^\circ$ ; (2) foot-flat – the foot is in full contact with the ground, while the ankle joint is in plantar flexion; (3) vertical-tibia – tibia is in a vertical position with neutral ankle angle ( $\theta_3 = 90^\circ$  and  $\varphi_3 = 0^\circ$ ); (4) heel-rise – the foot is in maximum dorsiflexion, and the heel rises from the ground; (5) plantar flexion onset – ankle starts plantar flexing and (6) toe-off – the foot loses contact with the ground.

The model calculates the vertical position ( $y_i$ ) of the knee for a given horizontal position ( $x_i$ ) of the knee. By combining the positions calculated for each event (see the following), the position of the knee for the whole duration of the stance phase is calculated by cubic hermite interpolation. The horizontal position is defined for each event as a percentage of the complete distance that is covered during stance phase (Appendix 2).

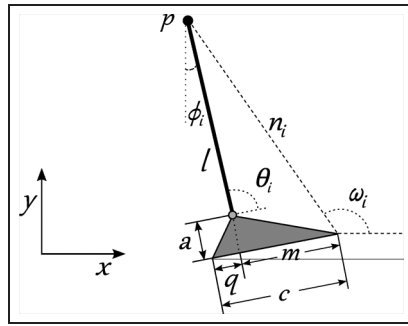


**Figure 2.** Graphical representation of the geometric model with indication of tibia length ( $l$ ), foot length ( $c$ ), ankle height ( $a$ ), the ankle–heel distance ( $q$ ), the dorsiflexion angle ( $\theta_i$ ), the angle of the tibia with the vertical direction ( $\varphi_i$ ). The angle  $\omega_i$  is an intermediate variable. The knee position ( $p$ ) is calculated by the model for six events of the gait cycle.

### 1. Heel-strike ( $x_1 = 0\%$ of stance phase)

The horizontal position of the knee at heel-strike is defined as  $x_1 = 0\%$ . The vertical position of the knee ( $y_1$ ) is calculated by the equation (1).

$$y_1 = l \cos \varphi_1 + \sqrt{q^2 + a^2} \cos \left( \theta_1 - \varphi_1 - \tan^{-1} \frac{a}{q} \right) \quad (1)$$

Based on reference normal gait data from our own lab and according to literature,<sup>12</sup> the parameters  $\varphi_1$  and  $\theta_1$  are defined as  $14^\circ$  and  $97^\circ$ , respectively.

### 2. Foot-flat ( $x_2 = 7\%$ of stance phase)

The motion between events 1 and 2 is represented by two simple rotations: (a) the rotation of the foot around the heel and (b) the rotation of the tibia around the ankle joint. The vertical displacement of the tibia induced by the first rotation is calculated by equation (2)

$$\Delta x_{2,1} = \sqrt{q^2 + a^2} \left( \cos \left( \tan^{-1} \frac{a}{q} \right) - \sin \left( \theta_1 - \varphi_1 - \tan^{-1} \frac{a}{q} \right) \right) \quad (2)$$

In order to calculate the vertical displacement of the knee at the foot-flat event after the second rotation, the angle between the tibia and ground at flat-foot ( $\varphi_2$ ) needs to be calculated by equation (3)

$$\varphi_2 = \sin^{-1} \left( \frac{\Delta x_{2,1} - x_2 + l \sin \varphi_1}{l} \right) \quad (3)$$

Thus, the vertical position of the knee at flat-foot is calculated by equation (4)

$$y_2 = a + l \cos \varphi_2 \quad (4)$$

### 3. Vertical-tibia

The motion of the knee between events 2 and 3 is a circular motion around the ankle joint. At the vertical-tibia event, the vertical position ( $y_3$ ) of the knee is defined from equation (5) and the horizontal ( $x_3$ ) from equation (6).

$$y_3 = l + a \quad (5)$$

$$x_3 = x_2 + l \sin \varphi_2 \quad (6)$$

### 4. Heel-rise ( $x_4 = 40\%$ of stance phase)

Between events 3 and 4, the circular motion continues. At the heel-rise event, the vertical position of the knee is therefore given by equation (7)

$$y_4 = a + \sqrt{l^2 - (x_4 - x_3)^2} \quad (7)$$

The amount of dorsiflexion at the moment of the heel-rise is calculated by the equation (8)

$$\theta_4 = \sin^{-1} \left( \frac{y_4 - a}{l} \right) \quad (8)$$

### 5. Plantar flexion onset ( $x_5 = 70\%$ of stance phase)

After the heel-rise, the tibia-foot complex rotates around the metatarso-phalangeal joint with a constant ankle angle. This phase ends with the plantar flexion onset. To mathematically describe the vertical position of the knee

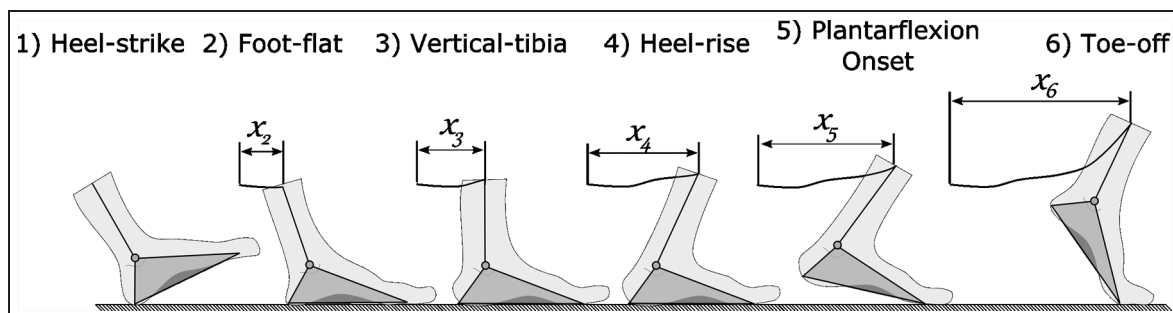


**Figure 3.** Events considered by the model.

at this event ( $y_5$ ), the distance between the knee and the metatarsal head is calculated by equation (9)

$$n_i = \sqrt{l^2 + m^2 + a^2 - 2l\sqrt{m^2 + a^2} \cos\left(\theta_i + \tan^{-1}\left(\frac{a}{m}\right)\right)} \quad (9)$$

where

$$m = c - q \quad (10)$$

and  $\theta_5 = \theta_4$ , since the ankle angle is constant. The vertical position of the knee at plantar flexion onset ( $y_5$ ) depends on the angle between the line  $n_i$  and the ground for events 4 and 5 given by equations (11) and (12), respectively

$$\omega_4 = \cos^{-1} \frac{n_4^2 + m^2 + a^2 - l^2}{2n_4\sqrt{m^2 + a^2}} + \tan^{-1} \frac{a}{m} \quad (11)$$

$$\omega_5 = \cos^{-1} \left( \frac{x_5 - x_4 + n_4 \cos \omega_4}{n_5} \right) \quad (12)$$

$$n_4 = n_5 \quad (13)$$

The vertical position of the knee at plantar flexion onset ( $y_5$ ) is then calculated by equation (14)

$$y_5 = n_5 \sin \omega_5 \quad (14)$$

#### 6. Toe-off ( $x_6 = 100\%$ of stance phase)

Between events 5 and 6, the foot rotates around the metatarso-phalangeal joint axis, while the tibia rotates around the ankle joint. At toe-off, the foot is in maximum plantar flexion ( $\theta_6 = 105^\circ$ ). The vertical position of the knee ( $y_6$ ) is calculated by equation (16). The length  $n_6$  is calculated from equation (9).

$$\omega_6 = \cos^{-1} \left( \frac{x_6 - x_5 + n_5 \cos \omega_5}{n_6} \right) \quad (15)$$

$$y_6 = n_6 \sin \omega_6 \quad (16)$$

#### Model implementation in the in vitro simulator set-up

The tibial kinematics model is implemented in a custom-made in vitro gait simulator based on previous studies.<sup>1,6-11</sup> The vertical position of the platform, that is, simulating the tibial kinematics in the vertical direction, is controlled by a pneumatic actuator (Festo ADNGF-63-100-P-A, Sankt Ingbert, Germany) that can deliver a maximum force of 2200 N in both directions. The position of the platform is measured with two position sensors (Festo SMAT 8E-550-IU-M8,  $\pm 0.064$  mm, 2 kHz), attached to the actuator. The position of the platform is controlled by a dedicated real-time engine that adapts the pressure in the chambers of the actuator accordingly. Since an upward displacement of the platform is equivalent to a downward displacement of the knee, the calculated vertical position should be inverted.

To achieve a normal role off, the controller needs to accurately fit the horizontal position of the carriage and the vertical position of the platform to set-points representative of the relative motion of the knee with respect to the ground during stance phase. However, as friction and compressibility of air in the pneumatic actuators induce high non-linearities, the dynamic position control of the platform is very complex. Therefore, a sophisticated control scheme, based on a solution proposed by Lee et al.,<sup>13</sup> was used. They suggest using a dual-loop proportional-integral-derivative (PID) controller, which was incorporated into the custom-made software programmed in LabVIEW v2009 (National Instruments, Austin, USA) that controls the operation of the simulator. The principle of operation of the controller is presented in Figure 4.

The outer loop of the PID controller compares in real time the measured vertical position of the platform ( $y$ ) with the desired set-point ( $y_r$ ) and estimates a pressure level that would minimise this difference ( $\Delta P_r$ ). This estimation accounts for the actuator friction and weight of the platform ( $w_p = 59$  kg). The direction of friction in the actuator is determined from the sign of the pressure difference between the two chambers of the actuator (friction is always opposite to the direction of the actuator force). The magnitude of friction is

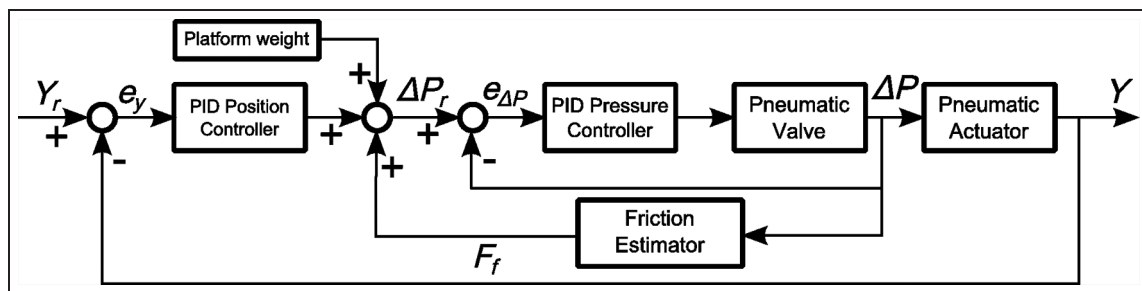


**Figure 4.** Dual-loop control scheme for position control of the platform: relationship between the measured position ( $y$ ), the measured pressure difference ( $\Delta P$ ), the position set-point ( $y_r$ ), the difference pressure set-point ( $\Delta P_r$ ) and the friction estimation ( $F_f$ ).

considered constant and equal to  $F_f = 10$  N based on measurements that were conducted on the actuator.

The pressure estimation is then used as a set-point for the inner loop of the PID controller and is compared to the measured pressure ( $\Delta P$ ). To minimise the difference, the inner loop controls the position of the actuator valve. This way, a fast and accurate control of the vertical position of the platform is ensured.

## Model validation

### Sensitivity analysis

In order to determine the most crucial factors that affect our model outcome and to determine the required accuracy for our in vitro gait simulation control inputs, a sensitivity analysis of the model output for all the model input parameters was performed. The initial values of the analysis were based on the average values of all the cadaveric specimens that were measured during the in vitro study. The maximum and minimum values that were used for the sensitivity analysis for each parameter were based on the standard deviation (Table 1).

Four geometric parameters were studied: tibia length ( $l$ ), foot length ( $c$ ), ankle height ( $a$ ) and ankle distance from the heel ( $q$ ). They were changed individually, and the effect on the model prediction was investigated. More specifically, for all six gait events, the difference in the prediction of the vertical position of the knee using a specimen-specific combination of parameter values was compared to the predicted value when using the average parameter values.

### In vivo measurements

In order to quantify the predictive accuracy of the geometric model, its performance was evaluated by comparing the tibial kinematics, calculated by the model, to the tibial kinematics measured during marker-based gait analysis in three healthy adult subjects (Vicon, Oxford, UK). These subjects presented a normal variation of the tibial and foot geometry (Table 2).

During the in vivo gait analysis, the three-dimensional (3D) position of retroreflective markers positioned at (1) medial malleolus, (2) lateral malleolus, (3) metatarsal head 1, (4) heel and (5) fibular head was measured at 250 Hz during stance phase. The geometric dimensions were calculated based on marker positions during a static measurement: foot length ( $c$ ) was calculated as the distance between the heel and metatarsal head 1, tibia length ( $l$ ) was calculated from the landmarks of lateral malleolus and fibula head and foot dimensions ( $a$  and  $q$ ) were calculated based on the landmarks on the heel and lateral malleolus. The fibular marker was chosen due to its constant visibility during stance phase. To validate the model, horizontal and vertical positions of the fibular marker measured during stance phase were compared to the model output.

The root mean square error (RMSE) value calculated between the predicted and measured knee position for each time point and normalised over the number of samples serves as an indicator of the average error of the model performance for the duration of the stance phase.

### In vitro gait simulations

The model performance for the in vitro experiments was analysed using the gait simulator. Six freshly frozen cadaveric feet were tested for different model parameters, and the correspondence between the resulting vertical ground reaction forces (vGRFs) and the ones measured in vivo was analysed.

## Results

### Sensitivity analysis

The results of the sensitivity analysis are presented in Table 3. The initial values of the model ( $a_o = 68$  mm,  $q_o = 47$  mm,  $c_o = 188$  mm and  $l_{1,o} = 531$  mm) were chosen based on methods described in the previous section. From Table 3, it can be seen that parameter  $q$  determines early stance, whereas parameter  $c$  has more significant effects in the late stance. Parameters  $a$  and  $l$

**Table 1.** Geometric dimensions as measured in six cadaveric specimens. All the relevant model dimensions are displayed. The mean and the standard deviation for each dimension are also calculated.

Specimen no.	Cadaveric specimen dimensions (mm)			
	Ankle height ( $a$ )	Ankle–heel distance ( $q$ )	Foot length ( $c$ )	Tibia length ( $l$ )
1	60	45	190	560
2	70	45	180	510
3	60	40	180	510
4	70	55	200	520
5	65	50	180	550
6	80	45	195	535
Mean	67.5	46.6	187.5	530.8
SD	7.5	5.1	8.8	21

SD: standard deviation.

**Table 2.** Measured dimensions of the subjects' feet and tibial geometry. All the relevant model dimensions are displayed for the three control subjects and for both the left and the right foot. The mean and the standard deviation for each dimension are also calculated.

Subject	Control subject dimensions (mm, left/right foot)			
	Ankle height ( $a$ )	Ankle–heel distance ( $q$ )	Foot length ( $c$ )	Tibia length ( $l$ )
1	58/62	94/91	214/216	417/411
2	60/44	60/72	183/182	352/364
3	59/56	92/95	208/206	351/346
Mean	56.9	84.3	202.2	373.9
SD	5.6	13.2	13.7	29.2

SD: standard deviation.

**Table 3.** Sensitivity of the model on its geometric parameters. The effect of the change in the vertical position prediction for each event, in relation to changes in each parameter, is reflected in each column.

Parameter		Difference of vertical position prediction for each event (mm)					
Initial value	Difference	Heel-strike	Foot-flat	Mid-stance	Heel-rise	End of rigid body	Toe-off
$a_0 = 68$ mm	+2 SD	15.88	15.96	16	16.65	18.48	18.36
	+1 SD	7.94	7.98	8	8.32	9.25	9.19
	–1 SD	–7.94	–7.98	–8	–8.19	–8.8	–8.77
	–2 SD	–15.88	–15.97	–16	–16.67	–18.57	–18.47
$q_0 = 47$ mm	+2 SD	1.21	–0.001	0	0	0	0
	+1 SD	0.6	0	0	0	0	0
	–1 SD	–0.6	0	0	0	0	0
	–2 SD	–1.21	0.001	0	0	0	0
$c_0 = 188$ mm	+2 SD	0	0	0	0	6.38	17.32
	+1 SD	0	0	0	0	3.19	8.72
	–1 SD	0	0	0	0	–3.21	–8.86
	–2 SD	0	0	0	0	–6.4	–17.86
$l_0 = 531$ mm	+2 SD	40.75	40.75	42	44.06	48.92	51.7
	+1 SD	20.37	20.37	21	22.09	24.64	26.09
	–1 SD	–20.37	–20.37	–21	–22.01	–24.3	–25.87
	–2 SD	–40.75	–40.75	–42	–44.36	–49.57	–52.88

SD: standard deviation.

have an effect, which is almost constant during stance phase. The most influential of all parameters in the model is the tibia length presenting the largest variability within the tested subjects. Not only is the range of values of tibia length clearly larger than the rest of the parameters, this parameter also affects the kinematics throughout the stance phase as well.

### *In vivo validation*

The comparison of the in vivo measurements in three subjects and the model predictions is presented in Figure 5. Both feet of the three subjects were used for the comparison.

For all measured subjects, good agreement is found between the predicted and measured tibial kinematics. The agreement is particularly good during the first stages of the stance phase (from the heel-strike to the heel-rise event), where the model is able to predict the position of the marker with an average accuracy of RMSE = 2.1 mm, while the average accuracy for the whole stance is RMSE = 3.1 mm.

### *In vitro validation*

In Figure 6, the results of the sensitivity of the in vitro simulations on the parameter  $q$  are presented. The parameter  $q$  was altered for one specimen deliberately from  $q = 0$  mm up to  $q = 40$  mm. The actual measured distance on the cadaveric specimen was  $q = 35$  mm. The resulting GRF is greatly affected by the changes on the control input by the parameter  $q$  with differences of up to 700 N. The closer the parameter approximates the actual dimension of the cadaveric specimen ( $q = 35$ ), the more physiological the GRF appears.

### **Discussion**

A geometric model that is able to predict sagittal plane motion of the knee during the stance phase of gait, taking into consideration only geometric parameters of the subjects' foot and tibia, was developed.

Currently, when performing in vitro gait studies, in vivo measurements of tibial kinematics are used directly as control inputs, creating several complications as reported by Whittaker et al.<sup>11</sup> and Sharkey

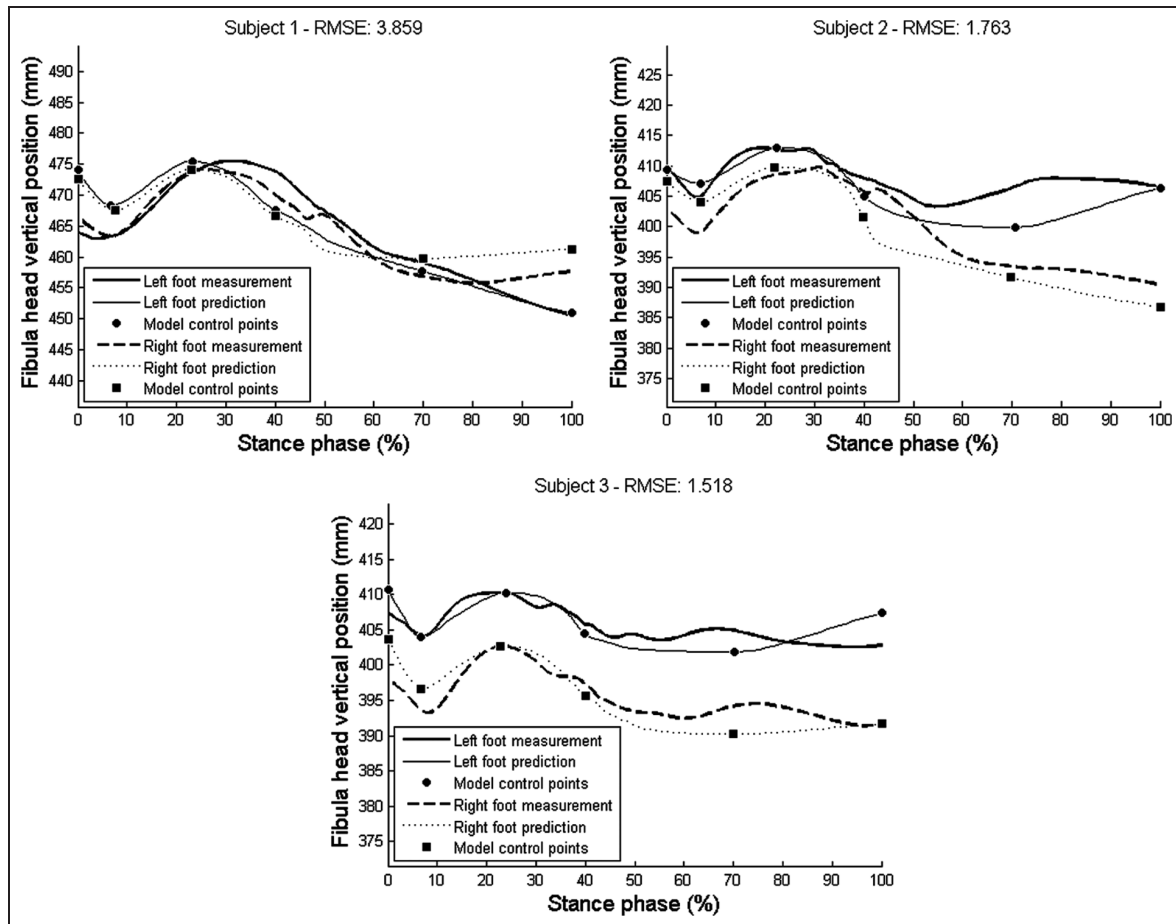


**Figure 5.** Comparison of model predicted (dashed lines) and the in vivo measured (continuous lines) trajectory of the fibula head marker for three subjects. The comparison was made for both left (thick lines) and right foot (thin lines) of the subject.

and Hamel.<sup>7</sup> It is shown that, by using a geometrical model, it is possible to account for the geometric dimensions of the cadaveric specimens, and to perform in vitro studies with different-sized specimens without the need for arbitrary tuning of the control input parameters.

Based on the sensitivity analysis of the model, it can be concluded that the geometric dimensions of the foot and tibia segments strongly affect the tibial kinematics. The most important parameter appears to be the tibia length ( $l$ ), exhibiting a difference of 20 mm in the prediction per 1 standard deviation (21 mm) difference in the parameter. Even though the effect seems larger than the other parameters, it is merely an offset imposition on the prediction, meaning that the effect of the change remains almost equal through the whole stance phase. However, a detailed analysis on the effect of the three remaining parameters reveals that they affect differently the different phases of the stance phase. This sensitivity analysis stresses the necessity of using a specimen specific control input for gait simulations even more, as it reveals that small differences on the dimensions of the specimens have a big effect on the tibial kinematics that can even differ between the different sub-phases of the stance.

By comparing the model output with the measured in vivo kinematics, it is shown that the model is able to predict the kinematics with a high accuracy, achieving RMSE values lower than 4 mm for control subjects who present a physiologic distribution in tibial and foot dimensions. Furthermore, an equally high performance of the model during the in vitro validation is shown, since physiological GRF can be generated over the complete stance phase of gait induced on the cadaveric specimens.

The presented method only predicts tibial kinematics in the sagittal plane. Given that most state-of-the-art simulators<sup>1,7-9</sup> allow controlling only horizontal and vertical tibial translation as well as knee flexion angle, this correction seems sufficient to accommodate for inter-specimen variability. The authors recognise that the absence of control of the tibial position in the frontal and transverse plane does not allow accounting for the interaction of foot pronation and tibial internal-external rotation. As such, the presented approach allows defining sagittal plane tibial kinematics that will induce a more physiologic 3D foot rollover, however, in the absence of frontal and transverse plane knee control. Although the model and the methods used are easy to transfer

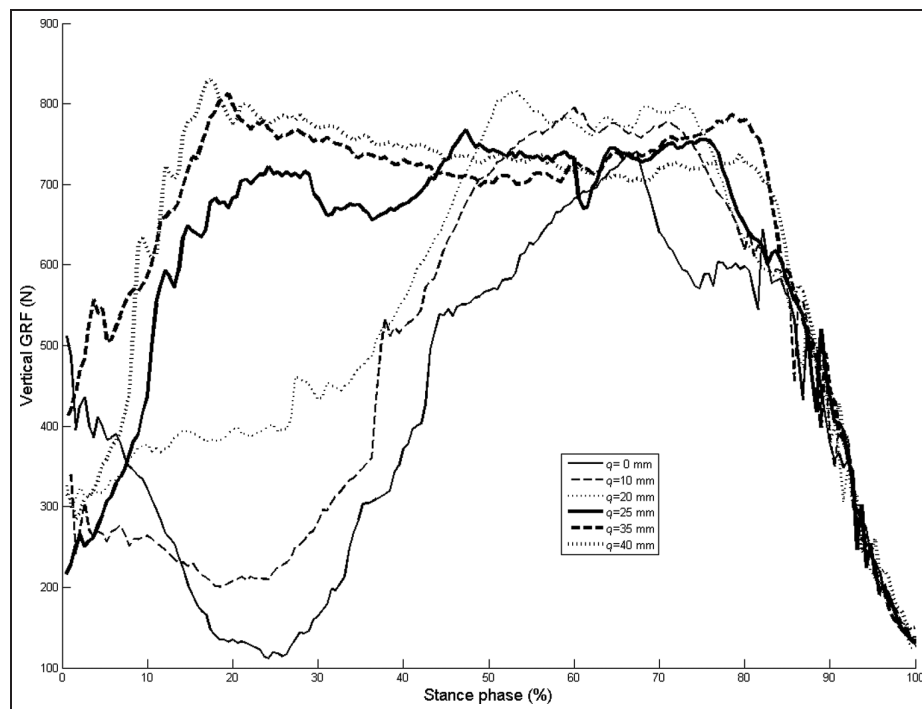


**Figure 6.** In vitro measured vertical GRF. The effect of a different value for the parameter  $q$  can be reflected on the measured vertical GRF. By approaching the measured value for the parameter, the vertical GRF appears more physiological, following the known 'M-shape'.

GRF: ground reaction force.

and implement in other gait simulators, the effect of including 3D tibial kinematics will need to be further explored.

## Conclusion

In this article, an innovative approach to generate the tibial kinematics control input for in vitro gait simulations is presented. Based on our findings, it can be concluded that the input parameters to the geometric model can be determined with sufficient accuracy in order to predict tibial kinematics in the sagittal plane. Furthermore, it was shown that the resulting GRF appears to be as physiologic as in in vivo measurements. As a result of this approach, arbitrary parameter tuning of the control variable of in vitro gait simulations is no longer required. This enhances the applicability of the in vitro gait simulations, even in specimens with rather extreme morphology.

## Funding

This work was funded by the Chair Berghmans-Dereymaeker, the Research Foundation Flanders and the Agency for Innovation by Science and Technology in Flanders (IWT).

## Conflict of interest

The authors have no conflicts of interest to report.

## References

1. Kyu-Jung K, Kitaoka HB, Luo Z-P, et al. In vitro simulation of the stance phase in human gait. *J Musculoskeletal Res* 2001; 5: 113–121.
2. Hamel AJ, Sharkey NA, Buczek FL, et al. Relative motions of the tibia, talus, and calcaneus during the stance phase of gait: a cadaver study. *Gait Posture* 2004; 20: 147–153.
3. Matricali GA, Bartels W, Labey L, et al. High interspecimen variability of baseline data for the tibio-talar contact area. *Clin Biomech* 2009; 24: 117–120.
4. Suckel A, Muller O, Wachter N, et al. In vitro measurement of intraarticular pressure in the ankle joint. *Knee Surg Sports Traumatol Arthrosc* 2010; 18: 664–668.
5. Suckel A, Muller O, Langenstein P, et al. Chopart's joint load during gait: in vitro study of 10 cadaver specimen in a dynamic model. *Gait Posture* 2008; 27: 216–222.
6. Burg J, Peeters K, Natsakis T, et al. In vitro analysis on the effect of muscle action on hind foot kinematics during stance. *J Biomech* 2012; 45: S190.
7. Sharkey NA and Hamel AJ. A dynamic cadaver model of the stance phase of gait: performance characteristics and kinetic validation. *Clin Biomech* 1998; 13: 420–433.
8. Hurschler C, Emmerich J and Wülker N. In vitro simulation of stance phase gait part I: model verification. *Foot Ankle Int* 2003; 24: 614–622.
9. Nester CJ, Liu AM, Ward E, et al. In vitro study of foot kinematics using a dynamic walking cadaver model. *J Biomech* 2007; 40: 1927–1937.
10. Noble LD, Colbrunn RW, Lee D-G, et al. Design and validation of a general purpose robotic testing system for

musculoskeletal applications. *J Biomech Eng* 2010; 132: 025001–025012.

11. Whittaker EC, Aubin PM and Ledoux WR. Foot bone kinematics as measured in a cadaveric robotic gait simulator. *Gait Posture* 2011; 33: 645–650.
12. Winter DA. *Biomechanics and motor control of human movement*. 4th ed. New York: Wiley-Interscience, 1990, p.384.
13. Lee HK, Choi GS and Choi GH. A study on tracking position control of pneumatic actuators. *Mechatronics* 2002; 12: 813–831.

## Appendix I

### Notation

$a$	ankle height from the ground
$c$	foot length
$e_y$	error between measured and imposed vertical position
$e_{\Delta P}$	error between measured and imposed pressure difference
$F_f$	friction estimation
$l$	tibia length
$m$	horizontal distance from heel to metatarsal head one
$n_i$	distance between knee and metatarsal head one
$p$	position of knee
$q$	horizontal distance of the ankle from the heel
$x_i$	horizontal position of the knee
$y_i$	vertical position of the knee
$y_r$	set-point for vertical position of the platform
$w_p$	weight of the platform
$\Delta P$	measured pressure difference of the actuator
$\Delta P_r$	set-point for the pressure difference of the actuator
$\theta_i$	dorsiflexion angle between the tibia and the foot
$\varphi_i$	angle between the tibia and the vertical
$\omega_i$	angle between line connecting the knee and metatarsal head one and the ground

## Appendix 2

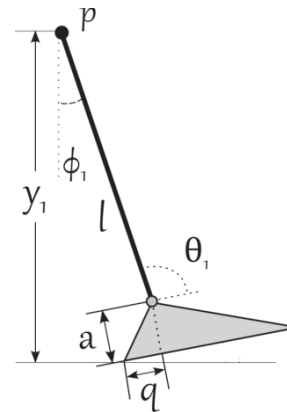
### Equations demonstration

The dimensions of two subjects (left feet of subject 1 and 2) are used for the demonstration of the calculations. The dimensions are

$$a_1 = 58 \text{ mm}, q_1 = 94 \text{ mm}, c_1 = 214 \text{ mm and } l_1 = 417 \text{ mm}$$

$$a_2 = 60 \text{ mm}, q_2 = 60 \text{ mm}, c_2 = 183 \text{ mm and } l_2 = 352 \text{ mm}$$

We also need to define the total knee translation for each specimen in the horizontal direction, which was measured in vivo to be  $x_1 = 480 \text{ mm}$  and  $x_2 = 422 \text{ mm}$ .

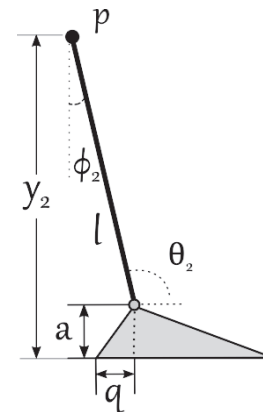


#### 1. Heel-strike

$$y_1 = l \cos \varphi_1 + \sqrt{q^2 + a^2} \cos \left( \theta_1 - \varphi_1 - \tan^{-1} \frac{a}{q} \right)$$

Introducing the values of  $a$  and  $q$  for specimen 1 and 2 in the above equation, we have the following results:

For specimen 1:  $y_1 = 472 \text{ mm}$ , for specimen 2:  $y_1 = 408 \text{ mm}$



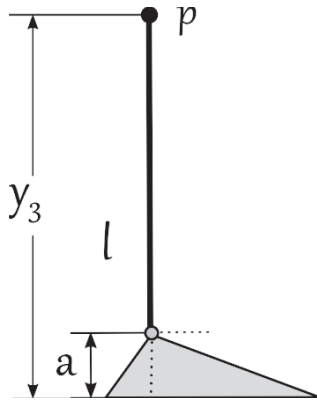
#### 2. Foot-flat

$$\Delta x_{2,1} = \sqrt{q^2 + a^2} \left( \cos \left( \tan^{-1} \frac{a}{q} \right) - \sin \left( \theta_1 - \varphi_1 - \tan^{-1} \frac{a}{q} \right) \right)$$

$$\varphi_2 = \sin^{-1} \left( \frac{\Delta x_{2,1} - x_2 + l \sin \varphi_1}{l} \right)$$

$$y_2 = a + l \cos \varphi_2$$

For specimen 1:  $\Delta x_{2,1} = 7.69 \text{ mm}$ ,  $\varphi_2 = 10.3^\circ$  and  $y_2 = 468 \text{ mm}$ . For specimen 2:  $\Delta x_{2,1} = 7.75 \text{ mm}$ ,  $\varphi_2 = 10.3^\circ$  and  $y_2 = 406 \text{ mm}$ .

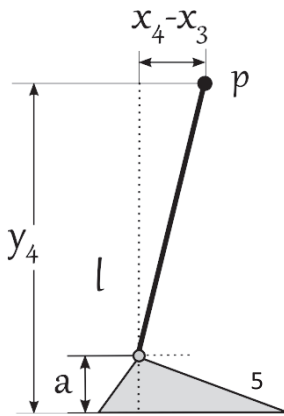


3. Vertical-tibia

$$y_3 = l + a$$

$$x_3 = x_2 + l \sin \varphi_2$$

For specimen 1:  $y_3 = 475$  mm and  $x_3 = 108$  mm. For specimen 2:  $y_3 = 412$  mm and  $x_3 = 93$  mm.

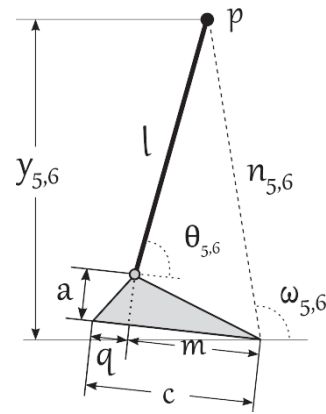


4. Heel-off

$$y_4 = a + \sqrt{l^2 - (x_4 - x_3)^2}$$

$$\theta_4 = \sin^{-1} \left( \frac{y_4 - a}{l} \right)$$

For specimen 1:  $y_4 = 466$  mm and  $\theta_4 = 78.4^\circ$ . For specimen 2:  $y_4 = 403$  mm and  $\theta_4 = 77.5^\circ$ .



5. Plantar flexion onset and toe-off

$$n_i = \sqrt{l^2 + m^2 + a^2 - 2l\sqrt{m^2 + a^2} \cos \left( \theta_i + \tan^{-1} \left( \frac{a}{m} \right) \right)}$$

$$m = c - q$$

$$\theta_5 = \theta_4 \text{ and } \theta_6 = 105^\circ$$

$$\omega_4 = \cos^{-1} \frac{n_4^2 + m^2 + a^2 - l^2}{2n_4\sqrt{m^2 + a^2}} + \tan^{-1} \frac{a}{m}$$

$$\omega_5 = \cos^{-1} \left( \frac{x_5 - x_4 + n_4 \cos \omega_4}{n_5} \right)$$

$$n_4 = n_5$$

$$y_5 = n_5 \sin \omega_5$$

$$\omega_6 = \cos^{-1} \left( \frac{x_6 - x_5 + n_5 \cos \omega_5}{n_6} \right)$$

$$y_6 = n_6 \sin \omega_6$$

For specimen 1:  $\omega_4 = 85.5^\circ$ ,  $\omega_5 = 103.2^\circ$ ,  $n_4 = n_5 = 468$  mm,  $y_5 = 455$  mm,  $\omega_6 = 119^\circ$  and  $y_6 = 448$  mm

For specimen 2:  $\omega_4 = 83.2^\circ$ ,  $\omega_5 = 101.2^\circ$ ,  $n_4 = n_5 = 406$  mm,  $y_5 = 398$  mm,  $\omega_6 = 117^\circ$  and  $y_6 = 404$  mm